A Loop Shaping Design Procedure Using H_∞ Synthesis

Duncan McFarlane, *Member, IEEE,* and Keith Glover, *Senior Member, IEEE*

Abstract—**A design procedure is introduced which incorporates loop shaping methods to obtain performance/robust stability tradeoffs, and a particular H_∞ optimization problem to guarantee closed-loop stability and a level of robust stability at all frequencies. Theoretical justification of this technique is given, and the effect of loop shaping on closed-loop behavior is examined. The procedure is illustrated in a controller design for a flexible space platform.**

I. Introduction to Loop Shaping Methods

A WELL-known approach to multiinput, multioutput (MIMO) feedback controller design is the so-called loop shaping approach (see [3], [17]), whereby a designer specifies *closed-loop* objectives in terms of requirements on the *open-loop* singular values, denoted $\sigma(\cdot)$, of the compensated system. Simplistically, by selecting a controller which achieves sufficiently high (respectively, low) open-loop gain at low (respectively, high) frequency, guarantees concerning closed-loop performance (respectively, robust stability) can be made at these frequencies.

For example, given a plant G and a controller K, then for good performance we require $\bar{\sigma}((I - GK)^{-1})$ and $\bar{\sigma}((I - GK)^{-1}G)$ to be small (particularly at low frequency) and for good robust stability properties we require $\bar{\sigma}(K(I - GK)^{-1})$ and $\bar{\sigma}(GK(I - GK)^{-1})$ to be small (at high frequency, in particular). Table I outlines some typical design objectives.

In loop shaping design, a designer specifies *closed-loop* objectives in terms of requirements on the *open-loop* singular values of the compensated system. For example, at frequencies such that $\underline{\sigma}(GK) \gg 1$, where $\underline{\sigma}(\cdot)$ denotes the minimum singular value, then the loop gain is large, and we can make the approximations

$$\bar{\sigma}\big((I - GK)^{-1}\big) \simeq 1/\underline{\sigma}(GK) \tag{1.1}$$

$$\bar{\sigma}\big((I - GK)^{-1}G\big) \simeq 1/\underline{\sigma}(K). \tag{1.2}$$

Further, if $\bar{\sigma}(GK) \ll 1$ (the loop gain is low), then

$$\bar{\sigma}\big(K(I - GK)^{-1}\big) \simeq \bar{\sigma}(K) \tag{1.3}$$

$$\bar{\sigma}\big(GK(I - GK)^{-1}\big) \simeq \bar{\sigma}(GK). \tag{1.4}$$

Manuscript received February 13, 1990; revised January 11, 1991 and October 8, 1991. Paper recommended by Associate Editor, J. Hammer.

D. McFarlane is with BHP Research, Melbourne Laboratories, Clayton, Australia.

K. Glover is with the Department of Engineering, University of Cambridge, Cambridge, England.

IEEE Log Number 9108279.

Noting that the closed-loop performance objectives in (1.1) and (1.2) are particularly important at low frequency, and that the closed-loop robust stability objectives in (1.3) and (1.4) are particularly important at high frequency, a typical closed-loop design specification can be illustrated as in Fig. 1. Equations (1.1)–(1.4) show that the desired closed-loop behavior can be achieved by manipulation of the open-loop gains $\bar{\sigma}(GK), \underline{\sigma}(GK)$. Additionally, it may be necessary to further adjust the singular values of K to satisfy requirements in (1.2) and (1.3). This open-loop shaping approach is complicated, however, by the need to ensure stability of the resulting closed-loop system. This requires that plant phase properties also be considered, and the loop shape can be shown to be limited by such stability requirements. This is examined in [1] for the SISO case, and in [3] and [5] for a MIMO extension. Further, these requirements are even more restrictive if the nominal plant has RHP poles or zeros. (See [15] for example.) The design methods in [9] and [10], for example, incorporate mid frequency open-loop phase manipulations to ensure closed-loop stability.

A loop-shaping approach that is somewhat simpler from the designer's point of view is that used the loop transfer recovery (LTR) method in LQG design. (See [11] and [3].) In this method, the designer specifies a desired singular value loop-shape, and the guaranteed stability properties of the LQG compensator ensure stability. LTR, however, cannot systematically deal with plants with RHP zeros (see [21]), although recent work [26] has presented an approach for adjusting the recovery procedure for the case of nonminimum phase plants. LTR is also limited in that it can only guarantee performance and robust stability properties at either plant input or plant output: that is the designer can specify, via loop shaping, *either* the closed-loop transfer functions $(I - GK)^{-1}$, $GK(I - GK)^{-1}$ associated with the plant output, *or* $(I - KG)^{-1}$, $KG(I - KG)^{-1}$ associated with the plant input.

Another approach to MIMO feedback controller design is H_∞ synthesis (see [4] and [25] for example) where, in contrast to open-loop shaping, the designer specifies closed-loop objectives in terms of requirements on the singular values of weighted *closed-loop* transfer functions, and a stabilizing controller is obtained which (optimally) satisfies these requirements. This *closed-loop shaping* approach has the feature that specifications apply at *all* frequencies, while, as mentioned above, open-loop shaping specifications are restricted to frequencies of low and high loop gain. (Refer to [18] for details of such a design procedure.) A difficulty with the H_∞ design approach is that the appropriate selection of

0018-9286/92$03.00 © 1992 IEEE

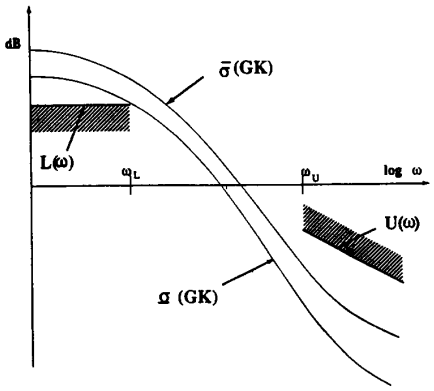

Fig. 1. Open-loop singular value shaping.

TABLE I
COMMON CLOSED-LOOP TRANSFER FUNCTION OBJECTIVES

Function	Interpretation
$\bar{\sigma}((I - GK)^{-1})$	—Gain from output disturbance to controller input. —Gain from reference signal to tracking error.
$\bar{\sigma}((I - KG)^{-1})$	—Gain from input disturbance to plant input.
$\bar{\sigma}(K(I - GK)^{-1})$	—Gain from output disturbance to controller output. —$1/\bar{\sigma}(K(I - GK)^{-1})$ indicates the maximum allowable additive plant perturbation for closed-loop stability.
$\bar{\sigma}((I - GK)^{-1}G)$	—Gain from input disturbance to plant output. —$1/\bar{\sigma}((I - GK)^{-1}G)$ indicates the maximum allowable additive controller perturbation for closed-loop stability.
$\bar{\sigma}(GK(I - GK)^{-1})$	—Gain from controller input disturbance to plant output. —$1/\bar{\sigma}(GK(I - GK)^{-1})$ indicates the maximum allowable output multiplicative plant perturbation for closed-loop stability.
$\bar{\sigma}(K(I - GK)^{-1}G)$	—Gain from input disturbance to controller output. —$1/\bar{\sigma}(K(I - GK)^{-1}G)$ indicates the maximum allowable input multiplicative plant perturbation for closed-loop stability.

closed-loop objectives and weights is not straightforward, and tends to be developed for each particular example. Further, by specifying requirements on *closed-loop* transfer functions it is possible for specifications to be made without regard for properties of the nominal plant. This can often be undesirable: for example, in [20] it is shown that some H_∞ design procedures produce controllers whose zeros cancel all the stable plant poles, which can be unacceptable when the plant contains lightly damped modes. H_∞ design methods have also been extended to the so-called *structured singular value* problem (see [2] or [19], for example), which allows closed-loop shaping of individual plant loops, giving the designer additional degrees of freedom in specifying a controller.

In this paper we present a design procedure, originally proposed in [12] and further developed in [13] and [14], which incorporates characteristics of both loop shaping and H_∞ design. Specifically, we make use of the so-called *normalized coprime factor H_∞ robust stabilization problem* which has been solved explicitly in [7], [8] and is equivalent to the gap metric robustness optimization as in [6]. The design technique has two main stages: 1) loop shaping is used to shape the nominal plant singular values to give desired open-loop properties at frequencies of high and low loop gain; 2) the normalized coprime factor H_∞ problem mentioned above is used to robustly stabilize this shaped plant.

The paper is structured in the following way. In Section II the design procedure is outlined, and in Section III we give theoretical justification for adopting this design approach. In Section IV we examine the effect of the selected loop shape on closed-loop behavior. In Section V we illustrate the design procedure in a design example.

II. THE DESIGN PROCEDURE

We will now formally state the design procedure that was proposed in the previous section. The objective of this approach is to incorporate the simple performance/robustness tradeoff obtained in loop shaping, with the guaranteed stability properties of H_∞ design methods. Theoretical justification for this technique will be given in the next section.

A. The Loop Shaping Design Procedure (LSDP)

1) Loop Shaping: Using a precompensator W_1 and/or a postcompensator W_2, the singular values of the nominal plant are shaped to give a desired open-loop shape. The nominal plant G and shaping functions W_1, W_2 are combined to form the shaped plant, G_S where $G_S = W_2 G W_1$. [See Fig. 2(a).] We assume that W_1 and W_2 are such that G_S contains no hidden modes.

2) Robust Stabilization: a) Calculate $\epsilon_{\max}$, where

$$\epsilon_{\max}^{-1} \triangleq \inf_{K \text{ stabilizing}} \left\| \begin{bmatrix} I \\ K \end{bmatrix} (I - G_S K)^{-1} \tilde{M}_S^{-1} \right\|_\infty$$

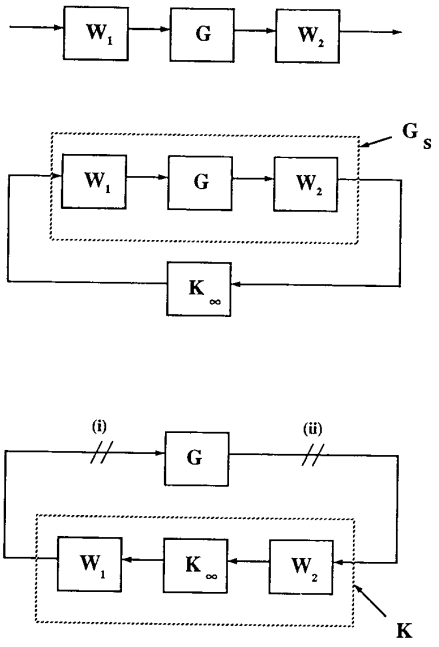

Fig. 2. The loop shaping design procedure.

and $\tilde{M}_s$, $\tilde{N}_s$ define the normalized coprime factors of G_S such that $G_S = \tilde{M}_s^{-1}\tilde{N}_s$ and $\tilde{M}_s\tilde{M}_s^* + \tilde{N}_s\tilde{N}_s^* = I$ and $\|\cdot\|_\infty$ denotes the H_∞ norm which is the supremum of the largest singular value over all frequencies. If $\epsilon_{\max} \ll 1$ return to 1) and adjust W_1 and W_2. b) Select $\epsilon \leq \epsilon_{\max}$, then synthesise a stabilizing controller K_∞, which satisfies

$$\left\| \begin{bmatrix} I \\ K_\infty \end{bmatrix} (I - G_S K_\infty)^{-1} \tilde{M}_s^{-1} \right\|_\infty \leq \epsilon^{-1}.$$

[See Fig. 2(b)].

3) The final feedback controller K is then constructed by combining the H_∞ controller K_∞ with the shaping functions W_1 and W_2 such that $K = W_1 K_\infty W_2$. [See Fig. 2(c).]

A typical design works as follows: the designer inspects the open-loop singular values of the nominal plant, and shapes these by pre- and/or postcompensation until nominal performance (and possibly robust stability) specifications are met. (Recall that the open-loop shape is related to closed-loop objectives.) A feedback controller K_∞ with associated stability margin (for the shaped plant) $\epsilon \leq \epsilon_{\max}$, is then synthesized. If $\epsilon_{\max}$ is small, then the specified loop shape is incompatible with robust stability requirements, and should be adjusted accordingly, then K_∞ is reevaluated.

Remark 2.1: The measure $\epsilon_{\max}$ is the *stability margin* for the so-called normalized coprime factor robust stability problem (see Section III-A), and therefore provides a robust stability guarantee for the closed-loop system. However, in this design procedure we are interpreting the measure $\epsilon_{\max}$ more generally as an *indicator* of the success of the loop shaping, where we note from [7], [8], $\epsilon_{\max} < 1$ always. A small value of $\epsilon_{\max}$ ($\epsilon_{\max} \ll 1$) in Stage 2) always indicates incompatibility between the specified loop shape, the nominal plant phase, and robust closed-loop stability. (We will justify this interpretation in Section III.)

Remark 2.2: Note that, in contrast to the classical loop shaping approach, the loop shaping here is done *without* explicit regard for the nominal plant phase information. That is, closed-loop stability requirements are disregarded at this stage. Also, in contrast with conventional H_∞ design, the robust stabilization is done *without* frequency weighting. The design procedure described here is both simple and systematic, and only assumes knowledge of elementary loop shaping principles on the part of the designer.

Remark 2.3: The above robust stabilization objective can also be interpreted as the more standard H_∞ problem formulation of minimizing the H_∞ norm of the frequency weighted gain from disturbances on the plant input and output to the controller input and output as follows.

$$\begin{aligned}
&\left\| \begin{bmatrix} I \\ K_\infty \end{bmatrix} (I - G_S K_\infty)^{-1} \tilde{M}_s^{-1} \right\|_\infty \\
&\quad = \left\| \begin{bmatrix} I \\ K_\infty \end{bmatrix} (I - G_S K_\infty)^{-1} \begin{bmatrix} I & G_S \end{bmatrix} \right\|_\infty \\
&\quad = \left\| \begin{bmatrix} W_2 \\ W_1^{-1} K \end{bmatrix} (I - GK)^{-1} \begin{bmatrix} W_2^{-1} & GW_1 \end{bmatrix} \right\|_\infty \\
&\quad = \left\| \begin{bmatrix} I \\ G_S \end{bmatrix} (I - K_\infty G_S)^{-1} \begin{bmatrix} I & K_\infty \end{bmatrix} \right\|_\infty \\
&\quad = \left\| \begin{bmatrix} W_1^{-1} \\ W_2 G \end{bmatrix} (I - KG)^{-1} \begin{bmatrix} W_1 & GW_2^{-1} \end{bmatrix} \right\|_\infty
\end{aligned}$$

where we have postmultiplied by $[\tilde{M}_s\ \tilde{N}_s]$ as in [8, remark 5.3], to go to the four-block problem, and [6, corollary 1] to interchange K_∞ and G_S. This shows how all the closed-loop objectives of Table I are incorporated. Note that since W_1 and W_2 are both in the feedback loop they may have poles and zeros on the imaginary axis without giving numerical or other problems.

III. Using ϵ as a Design Indicator

The objective of this section is to provide justification for the use of parameter ϵ as a design indicator. We will show that ϵ is a measure of both closed-loop robust stability and the success of the design in meeting the loop shaping specifications.

A. Guarantees on Robust Stability

We will first show that ϵ provides robust stability guarantees for the closed-loop system.

The main results of [7], [8] for the normalized LCF robust stabilization H_∞ problem are now summarized. It has been shown [22], [23], [24], [6] that an attractive way of representing unstructured uncertainty in a plant is via coprime factor perturbations. That is, if the nominal plant is

$$G = \tilde{M}^{-1}\tilde{N} \tag{3.1}$$

then a perturbed plant (see Fig. 3) is written

$$G_\Delta = (\tilde{M} + \Delta_M)^{-1}(\tilde{N} + \Delta_N) \tag{3.2}$$

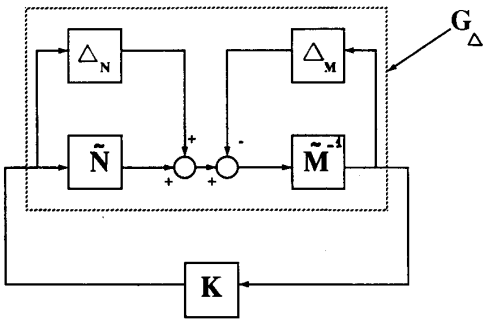

Fig. 3. Coprime factor robust stabilization problem.

where $\tilde{M}$, $\tilde{N}$ is a left coprime factorization (LCF) of G, and Δ_M, Δ_N are stable, unknown transfer functions representing the uncertainty and satisfying $\|[\Delta_M, \Delta_N]\|_\infty < \epsilon$ where $\epsilon > 0$. A design objective is then to find a feedback controller K which stabilizes all such G_Δ for a given ϵ. Following [24], this can be rewritten in the framework of an H_∞ optimization problem. Find a stabilizing controller K such that

$$\left\| \begin{bmatrix} (I - GK)^{-1}\tilde{M}^{-1} \\ K(I - GK)^{-1}\tilde{M}^{-1} \end{bmatrix} \right\|_\infty \leq \epsilon^{-1} \tag{3.3}$$

where K is chosen over all controllers which stabilize G. That is, a controller K is chosen so that it stabilizes the nominal plant, and satisfies the requirement on the H_∞ norm of the combination of closed-loop transfer functions in (3.3). The solution for the largest achievable ϵ $(= \epsilon_{\max})$ is generally iterative [24], *but* if the left coprime factorization (LCF) of G is *normalized*, meaning

$$\tilde{M}(j\omega)\tilde{M}(j\omega)^* + \tilde{N}(j\omega)\tilde{N}(j\omega)^* = I \qquad \text{for all } \omega \tag{3.4}$$

then it is possible to show [7], [8] that a maximum value of ϵ can be obtained by a noniterative method, and is given by

$$\epsilon_{\max} = \left(1 - \|[\tilde{M}, \tilde{N}]\|_H^2\right)^{1/2} \tag{3.5}$$

where $\|\cdot\|_H$ denotes the Hankel norm, and $\epsilon_{\max}$ is called the *maximum stability margin*.

A stabilizing controller achieving $\epsilon = \epsilon_{\max}$ is called an *optimal controller* for this problem, and a controller achieving $\epsilon < \epsilon_{\max}$ in (3.3) is referred to as a *suboptimal controller*.

In the context of the design procedure in Section II the results of this section provide a guarantee of robust stability in terms of perturbations to the coprime factors of the shaped plant.

B. Guarantees on the Achieved Loop Shape

In Section II we specified the desired loop shape by W_2GW_1 [Fig. 2(a)]. But, after Stage 2) of the design procedure, the actual loop shape achieved is in fact given by $W_1K_\infty W_2G$ at plant input [point i), Fig. 2(c)] and $GW_1K_\infty W_2$ at plant output [point ii), Fig. 2(c)]. It is therefore possible that the inclusion of K_∞ in the open-loop transfer function will cause deterioration in the open-loop shape specified by G_S. In this section, we will show that the degradation in the loop shape caused by the H_∞ controller K_∞ is limited at frequencies where the specified loop shape is sufficiently large or sufficiently small. In particular, in Theorem 3.1 and Corollary 3.2 we will show that at frequencies of high loop gain the *decrease* in loop gain due to the inclusion of K_∞ is limited, and in Theorem 3.3 and Corollary 3.4 we will show that at frequencies of low loop gain the *increase* in loop gain due to the inclusion of K_∞ is also limited.

We first examine the possibility of loop shape deterioration at frequencies of high loop gain (typically low frequency). At low frequency (in particular, $\omega \in (0, \omega_l)$ in Fig. 1), the deterioration in loop shape at plant output can be obtained by comparing $\underline{\sigma}(GW_1K_\infty W_2)$ to $\underline{\sigma}(W_2GW_1)$. Note that

$$\underline{\sigma}(GK) = \underline{\sigma}(GW_1K_\infty W_2) \geq \underline{\sigma}(W_2GW_1)\underline{\sigma}(K_\infty)/c(W_2), \tag{3.6}$$

where $c(\cdot)$ denotes condition number. Similarly, for loop shape deterioration at plant input, we compare $\underline{\sigma}(W_1K_\infty W_2G)$ to $\underline{\sigma}(W_2GW_1)$ and we have

$$\underline{\sigma}(KG) = \underline{\sigma}(W_1K_\infty W_2G) \geq \underline{\sigma}(W_2GW_1)\underline{\sigma}(K_\infty)/c(W_1). \tag{3.7}$$

In each case, $\underline{\sigma}(K_\infty)$ is required to obtain a bound on the deterioration in the loop shape at low frequency. Note that the condition numbers $c(W_1)$ and $c(W_2)$ are selected by the designer.

Next, recalling that G_S denotes the shaped plant, and that K_∞ robustly stabilizes the normalized coprime factorization of G_S with stability margin ϵ, then by (3.3) we have

$$\left\| \begin{bmatrix} K_\infty \\ I \end{bmatrix} (I - G_SK_\infty)^{-1}\tilde{M}_s^{-1} \right\|_\infty \leq \epsilon^{-1} \triangleq \gamma \tag{3.8}$$

where $(\tilde{N}_s, \tilde{M}_s)$ is a normalized LCF of G_S, and the parameter γ is defined to simplify the notation to follow. The following result shows that $\underline{\sigma}(K_\infty)$ is explicitly bounded by functions of ϵ and $\underline{\sigma}(G_S)$, the minimum singular value of the shaped plant, and hence by (3.6) and (3.7) K_∞ will only have a limited effect on the specified loop shape at low frequency.

Theorem 3.1: Any controller K_∞ satisfying (3.8), where G_S is assumed square, also satisfies

$$\underline{\sigma}(K_\infty(j\omega)) \geq \frac{\underline{\sigma}(G_S(j\omega)) - (\gamma^2 - 1)^{1/2}}{\sqrt{\gamma^2 - 1}\,\underline{\sigma}(G_S(j\omega)) + 1}$$

for all ω such that

$$\underline{\sigma}(G_S(j\omega)) > \sqrt{\gamma^2 - 1}\,.$$

Proof: (See Appendix I.)

The main implication of Theorem 3.1 is that the bound on $\underline{\sigma}(K_\infty)$ depends only on the selected loop shape, and the stability margin of the shaped plant. The value of $\gamma(= \epsilon^{-1})$ directly determines the frequency range over which this result is valid—a small γ (large ϵ) is desirable, as we would expect. Further, if we consider those frequencies where

$\underline{\sigma}(G_S) \gg \sqrt{\gamma^2 - 1}$, we have the following asymptotic result, which is immediate from Theorem 3.1.

Corollary 3.2: Following the notation of Theorem 3.1, if $\underline{\sigma}(G_S(j\omega)) \gg \sqrt{\gamma^2 - 1}$, then $\underline{\sigma}(K_\infty(j\omega)) \gtrsim (1/\sqrt{\gamma^2 - 1})$, where $\gtrsim$ denotes asymptotically greater than or equal to as $\underline{\sigma}(G_S) \to \infty$.

Corollary 3.2 simply states that if G_S has a sufficiently large loop gain, then so also will $G_S K_\infty$ provided $\gamma\ (= \epsilon^{-1})$ is sufficiently small.

In an analogous manner, we now examine the possibility of deterioration in the loop shape at high frequency due to the inclusion of K_∞. Note that at high frequency (in particular, $\omega \in (\omega_u, \infty)$ in Fig. 1) the deterioration in plant output loop shape can be obtained by comparing $\bar{\sigma}(GW_1K_\infty W_2)$ to $\bar{\sigma}(W_2GW_1)$. Note that, analogously to (3.6) and (3.7) we have

$$\bar{\sigma}(GK) = \bar{\sigma}(GW_1K_\infty W_2) \le \bar{\sigma}(W_2GW_1)\bar{\sigma}(K_\infty)c(W_2).$$

Similarly, the corresponding deterioration in plant input loop shape is obtained by comparing $\bar{\sigma}(W_1K_\infty W_2G)$ to $\bar{\sigma}(W_2GW_1)$ where

$$\bar{\sigma}(KG) = \bar{\sigma}(W_1K_\infty W_2G) \le \bar{\sigma}(W_2GW_1)\bar{\sigma}(K_\infty)c(W_1).$$

Hence, in each case, $\bar{\sigma}(K_\infty)$ is required to obtain a bound on the deterioration in the loop shape at high frequency. In an identical manner to Theorem 3.1, we now show that $\bar{\sigma}(K_\infty)$ is explicitly bounded by functions of γ, and $\bar{\sigma}(G_S)$, the maximum singular value of the shaped plant.

Theorem 3.3: Any controller K_∞ satisfying (3.8) also satisfies

$$\bar{\sigma}(K_\infty(j\omega)) \le \frac{(\gamma^2 - 1)^{1/2} + \bar{\sigma}(G_S(j\omega))}{1 - (\gamma^2 - 1)^{1/2}\bar{\sigma}(G_S(j\omega))}$$

for all ω such that

$$\bar{\sigma}(G_S(j\omega)) < \frac{1}{\sqrt{\gamma^2 - 1}}.$$

(The proof of Theorem 3.3 closely follows that of Theorem 3.1, using a similar completion of the squares approach. The proof is therefore excluded here.)

Again, if we consider those frequencies at which $\bar{\sigma}(G_S) \ll (1/\sqrt{\gamma^2 - 1})$, then we have the following result, which is immediate from Theorem 3.3, and analogous to Corollary 3.2.

Corollary 3.4: Following the notation of Theorem 3.3, if $\bar{\sigma}(G_S(j\omega)) \ll (1/\sqrt{\gamma^2 - 1})$, then $\bar{\sigma}(K_\infty(j\omega)) \lesssim \sqrt{\gamma^2 - 1}$, where $\lesssim$ denotes asymptotically less than or equal to as $\bar{\sigma}(G_S) \to 0$.

Remark 3.5: The results in Corollaries 3.2 and 3.4 confirm that γ (alternatively ϵ) indicates the compatibility between the specified loop shape and closed-loop stability requirements.

We have shown in this section that the values of γ (alternatively ϵ) achieved in the loop shaping design procedure will directly affect the singular values of the H_∞ controller K_∞.

C. Assessing Any Stabilizing Controller Using ϵ

In Section III-A it was shown that the selection of a controller achieving a particular ϵ implies that specific robust stability guarantees exist and in Section III-B we evaluated bounds on the *maximum* loop shape deterioration at low and high loop gains, for a given $\epsilon(= \gamma^{-1})$, showing that the achieved loop shape can differ from the specified loop shape by only a limited amount. That is, a large value of ϵ leads to a successful loop shaping design. In this section we take a contrary approach: for a controller achieving a *small* stability margin, that is $\epsilon \ll 1$, is it *still* possible to guarantee that the final design has good robust stability properties and that a loop shape close to the specified loop shape has been achieved? That is, does a small value of ϵ *necessarily* lead to an unsuccessful loop shaping design? To show that this is the case, we note from Section III-A that, given any stabilizing controller K_a there exists a frequency ω_o such that

$$\bar{\sigma}\left(\begin{bmatrix} K_a \\ I \end{bmatrix}(I - G_SK_a)^{-1}\tilde{M}_s^{-1}\right)(j\omega_o) = \gamma \ge \gamma_{\min}.$$

We can now evaluate the *minimum* loop shape deterioration that can be expected, if any, for this γ, and examine the effect of γ on robust stability at this frequency. These ideas are summarized in the following theorem.

Theorem 3.6: Let $\epsilon_{\max} = \gamma_{\min}^{-1}$ be the optimal stability margin for the normalized coprime factor robust stabilization problem as given in (3.5). Then, for any stabilizing controller K_a there exists a frequency ω_o such that

$$\bar{\sigma}\left(\begin{bmatrix} K_a \\ I \end{bmatrix}(I - G_SK_a)^{-1}\tilde{M}_s^{-1}\right)(j\omega_o) \ge \gamma_{\min} \quad (3.9)$$

and hence:

i) there exists a perturbed system

$$G_\Delta = W_2^{-1}(\tilde{M}_s + \Delta_M)^{-1}(\tilde{N}_s + \Delta_N)W_1^{-1} \quad (3.10)$$

with

$$\|[\Delta_N, \Delta_M]\|_\infty \le \gamma_{\min}^{-1} \quad (3.11)$$

which destabilizes the system. Further:

ii) if $\underline{\sigma}(G_S(j\omega_o)) > (\gamma_{\min}^2 - 1)^{-1/2}$, then

$$\underline{\sigma}(K_a(j\omega_o)) \le \frac{(\gamma_{\min}^2 - 1)^{1/2} + \underline{\sigma}(G_S(j\omega_o))}{(\gamma_{\min}^2 - 1)^{1/2}\underline{\sigma}(G_S(j\omega_o)) - 1} \quad (3.12)$$

and

iii) if $\bar{\sigma}(G_S(j\omega_o)) < (\gamma_{\min}^2 - 1)^{1/2}$, then

$$\bar{\sigma}(K_a(j\omega_o)) \ge \frac{(\gamma_{\min}^2 - 1)^{1/2} - \bar{\sigma}(G_S(j\omega_o))}{(\gamma_{\min}^2 - 1)^{1/2}\bar{\sigma}(G_S(j\omega_o)) + 1}. \quad (3.13)$$

Proof: (See the Appendix.)

Remark 3.7: Theorem 3.6 states that, for any $\epsilon \le \epsilon_{\max}$, there will be a *minimum* deterioration in the desired loop shape at frequencies of high or low loop gain or there will exist a perturbation satisfying (3.11) which destabilizes the closed-loop system. This result shows that γ/ϵ is a design

indicator for the entire frequency range, as summarized below.

1) If the coprime factor robust stability is poor (that is, $\epsilon \ll 1$ or $\gamma \gg 1$) at a frequency where $\tilde{N}_s$ and $\tilde{M}_s$ are of comparable size, then i) shows that only a small relative perturbation on either $\tilde{N}_s$ or $\tilde{M}_s$ is permitted.

2) If $\tilde{M}_s \gg \tilde{N}_s$, then the notional destabilizing perturbation could correspond to a very large relative perturbation in N_s, implying that robust stability properties may in fact be acceptable despite $\gamma \gg 1$. However, in this case, we have $\bar{\sigma}(G_S) \ll 1$ and part iii) of Theorem 3.6 applies, showing that the loop gain is necessarily and undesirably increased.

3) If $\tilde{M}_s \ll \tilde{N}_s$, then the notational destabilizing perturbation could correspond to a very large relative perturbation in M_s, again implying that robust stability properties may in fact be acceptable despite $\gamma \gg 1$. However, in this case, we have $\underline{\sigma}(G_S) \gg 1$ and part ii) of Theorem 3.6 applies, showing that the loop gain is necessarily and undesirably decreased.

IV. Shaping Functions and Closed-Loop Behavior

The shaping functions W_1 and W_2 are used by the designer to make performance/robust stability tradeoffs in design. In this section we examine the effect of the shaping functions, W_1 and W_2, on closed-loop behavior.

A. Bounds on the Normalized Coprime Factors

We first state a technical result which demonstrates that $\bar{\sigma}(\tilde{N}_s)$ and $\bar{\sigma}(\tilde{M}_s)$ are related to the nominal plant G and the shaping functions W_1 and W_2.

Lemma 4.1: Let the shaped plant $G_S = W_2GW_1$ have a normalized LCF, respectively, RCF, given by $(\tilde{N}_s, \tilde{M}_s)$, respectively, (N_s, M_s). Then

$$\bar{\sigma}(\tilde{N}_s) = \bar{\sigma}(N_s) = \left(\frac{\bar{\sigma}^2(W_2GW_1)}{1+\bar{\sigma}^2(W_2GW_1)}\right)^{1/2} \quad (4.1)$$

and

$$\bar{\sigma}(\tilde{M}_s) = \bar{\sigma}(M_s) = \left(\frac{1}{1+\underline{\sigma}^2(W_2GW_1)}\right)^{1/2}. \quad (4.2)$$

Proof: Note, that by the definition of the normalized LCF in (3.4) and $G_S = W_2GW_1$ we have

$$\tilde{M}_s\tilde{M}_s^* = I - \tilde{N}_s\tilde{N}_s^* \quad (4.3)$$

$$\Rightarrow \tilde{M}_s^*\tilde{M}_s = \left(I + W_2GW_1W_1^*G^*W_2^*\right)^{-1}. \quad (4.4)$$

The remainder of the proof is straightforward and is omitted here. △△

B. Behavior of Standard Closed-Loop Objectives

In Section I we stated that a feature of the classical loop shaping design approach is that it is possible to ensure, by open-loop shaping, that a number of standard closed-loop design objectives are bounded. The following result demonstrates that this is also the case for the loop shaping design procedure outlined in Section II, and we obtain bounds on each closed-loop objective listed in Table I.

Theorem 4.2: Let G be the nominal plant and let $K = W_1K_\infty W_2$ be the associated controller obtained from the loop shaping design procedure of Section II. Then if

$$\left\| \begin{bmatrix} K_\infty \\ I \end{bmatrix} (I - G_SK_\infty)^{-1}\tilde{M}_s^{-1} \right\|_\infty \le \gamma$$

we have

$$\bar{\sigma}\left(K(I-GK)^{-1}\right) \le \gamma\bar{\sigma}(\tilde{M}_s)\bar{\sigma}(W_1)\bar{\sigma}(W_2) \quad (4.5)$$

$$\bar{\sigma}\left((I-GK)^{-1}\right) \le \min\left\{\gamma\bar{\sigma}(\tilde{M}_s)c(W_2), 1+\gamma\bar{\sigma}(N_s)c(W_2)\right\} \quad (4.6)$$

$$\bar{\sigma}\left(K(I-GK)^{-1}G\right) \le \min\left\{\gamma\bar{\sigma}(\tilde{N}_s)c(W_1), 1+\gamma\bar{\sigma}(M_s)c(W_1)\right\} \quad (4.7)$$

$$\bar{\sigma}\left((I-GK)^{-1}G\right) \le \frac{\gamma\bar{\sigma}(\tilde{N}_s)}{\underline{\sigma}(W_1)\underline{\sigma}(W_2)} \quad (4.8)$$

$$\bar{\sigma}\left((I-KG)^{-1}\right) \le \min\left\{1+\gamma\bar{\sigma}(\tilde{N}_s)c(W_1), \gamma\bar{\sigma}(M_s)c(W_1)\right\} \quad (4.9)$$

$$\bar{\sigma}\left(G(I-KG)^{-1}K\right) \le \min\left\{1+\gamma\bar{\sigma}(\tilde{M}_s)c(W_2), \gamma\bar{\sigma}(N_s)c(W_2)\right\} \quad (4.10)$$

where $(\tilde{N}_s, \tilde{M}_s)$, respectively, (N_s, M_s), is a normalized LCF, respectively, RCF, of $G_S = W_2GW_1$, and $c(\cdot)$ denotes $\bar{\sigma}(\cdot)/\underline{\sigma}(\cdot)$, the frequency-dependent condition number.

Proof: The proof of this theorem follows from simple matrix manipulation.

Remark 4.3: Note that, because $(\tilde{N}_s, \tilde{M}_s)$ is a *normalized* LCF of G_S, we have that $\bar{\sigma}(\tilde{N}_s) \le 1$ and $\bar{\sigma}(\tilde{M}_s) \le 1$ for all frequencies, and similar observations can be made for the normalized RCF case. Noting also that γ has a finite value (typically $2 < \gamma < 10$ in practice), and that the shaping functions are selected by the designer, then it can be seen that, by (4.5)–(4.10), all of the closed-loop objectives are guaranteed to have bounded magnitude. We say that in this case the objectives are *well behaved*.

Remark 4.4: In Theorem 4.2 we showed that the behavior of a number of different closed-loop transfer functions is dependent on the normalized LCF or normalized RCF of G_S. Combining these results with Lemma 4.1, the bounds on the closed-loop objectives in Theorem 4.2 can be rewritten in terms of γ, G, W_1, and W_2 only.

V. Attitude Control of a Flexible Space Platform

We now give a design example to illustrate the use of the design procedure presented in Section II.

A. The Dynamic Model

The model being considered in this example is a simplified finite element model (MIMO) of a large space platform. The model was supplied by Dr. M. Noton of the Space and Communications Division, British Aerospace P.L.C., and is intended to be generally representative of future large flexible

spacecraft. This system has been previously considered in [12], and the results presented in this section are an extension of that work (see [14] for further numerical details).

This elemental model is illustrated in Fig. 4 as an assembly point masses connected by massless struts exhibiting bending and torsional stiffnesses. The principal flexible effects arise from the solar arrays and the torsion of the main beam along the x-axis. This model has many modes but the studies have been restricted to rotations about the X and Z axes (roll and yaw) because the rotations about the Y axis (pitch) are decoupled and their control is simpler. The control variables shown in Fig. 4 are as follows:

u_1, u_2—torques by reaction wheel in centerbody

u_3, u_4—on-off thrusters at payloads P9 and P10.

The thrusters operate in an on-off mode but they have been treated as continuous linear actuators because they can be time modulated in a short sample interval. Measurements are as below:

y_1, y_2—roll and yaw angles at the centerbody (infrared sensors);

y_3, y_4—roll and yaw rates at the centerbody (rate gyros);

y_5—roll rate at P9 (rate gyro).

Modal cost analysis (see [16]) indicated that only five flexible modes need be considered and these tests were further restricted to the three most influential modes. The model has therefore 4 inputs, 5 outputs, and 10 states corresponding to 2 rigid body and 3 flexible modes. The nominal natural frequencies of the three flexible modes were $\omega_1 = 0.345$ rad/s, $\omega_2 = 0.531$ rad/s, and $\omega_3 = 0.762$ rad/s.

In practice, effective stiffnesses can be predicted only approximately beforehand, and the structures cannot be tested adequately on the ground. Therefore, in order to represent this uncertainty by a perturbed model the finite element analysis was repeated with a different principal stiffness, leading to significantly different modal frequencies, state, and measurement matrices. Damping of the modes does not come from the finite element analysis and is notoriously difficult to predict; it was set at not more than 1% for all modes.

B. Design Objectives

The two primary objectives of this design are robust stabilization and disturbance rejection. More specifically, because the actual stiffness of the platform are postulated to be very uncertain, it is desired to robustly stabilize the plant for a range of stiffnesses, and to ensure that the closed-loop damping is at an acceptable level. In addition, it is also desirable to minimize the effects of disturbances on outputs y_1 and y_2 (representing the angular positions of the platform) subject to constraints on peak inputs. The nominal specifications were therefore as follows.

1) Robust Stability: Stabilize nominal and perturbed plants and ensure damping $> 5\%$ always.

2) Disturbance Rejection: For $0.1Nm$ step inputs on u_1, u_2, ensure the maximum deflections satisfy $y_1, y_2 \leq 0.01°$.

3) Input Magnitudes: For $0.1Nm$ step inputs on u_1, u_2, ensure the maximum control signals satisfy u_1, $u_2 \leq 1.0Nm$ u_3, $u_4 \leq 0.5N$.

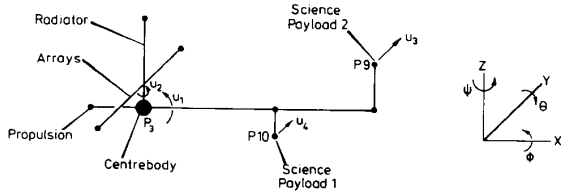

Fig. 4. Elementary model of a spacecraft.

These are based on specifications set in current designs.

In the interests of good control the closed-loop bandwidth was permitted to embrance the flexible modes. This generally creates difficulties, but as is shown in this design, can lead to superior performance characteristics. Zero steady-state deflections due to disturbances were also desired.

C. The Loop Shaping Design Procedure

In total, five designs were produced for this problem, and all were satisfactory according to the specifications, their bandwidth and steady-state properties being improved each time, while ensuring that robust stability and control energy requirements were satisfied. The final design is now described.

1) Loop Shaping: Inspection of the maximum singular value plot of the nominal plant [Fig. 5(a)] indicated that considerable additional gain was required to improve performance characteristics, especially the closed-loop bandwidth. Note that the nominal open-loop crossover frequency at ≈ 0.005 rad/s implies a very low closed-loop bandwidth. Gain of $\alpha = 4200$ in each output channel gave an open-loop gain crossover frequency of ≈ 1 rad/s for the shaped plant. [See Fig. 5(b).] Simple PI compensators of the form

$$W_c(s) = \frac{s + 0.1}{s}$$

were also added to output channels y_1 and y_2 to ensure zero steady-state output due to disturbances in these channels. The motivation behind this selection is that by (4.1) we have that, at frequencies of high loop gain (low frequency), $\bar{\sigma}(\tilde{N}_s) \simeq 1$, and by (4.8) this implies

$$\bar{\sigma}\left((I - GK)^{-1}G\right) \lesssim 1/\left(\underline{\sigma}(W_1)\underline{\sigma}(W_2)\right).$$

The shaped plant G_S was chosen to be of the form $G_S = W_2G$ where

$$W_2 = \text{diag}\left\{4200W_c; 4200W_c; 4200I_3\right\}.$$

The singular values of G_S are shown in Fig. 5(b).

2) Robust Stabilization: A controller K_∞ which robustly stabilized the normalized LCF of G_S was generated and a stability margin $\epsilon = 0.238$ was obtained. By Theorems 3.1 and 3.3, this indicated that deterioration in high and low frequency loop shapes was asymptotically no greater than a factor of 4 and that acceptable robust stability properties in the crossover frequency region were expected. Model reduction was then performed on G_S as in [14], and two states were removed. K_∞ was therefore a 10 state system.

3) Finally the H_∞ controller, K_∞ was cascaded with the shaping function W_2 to form the final controller $K = K_\infty W_2$

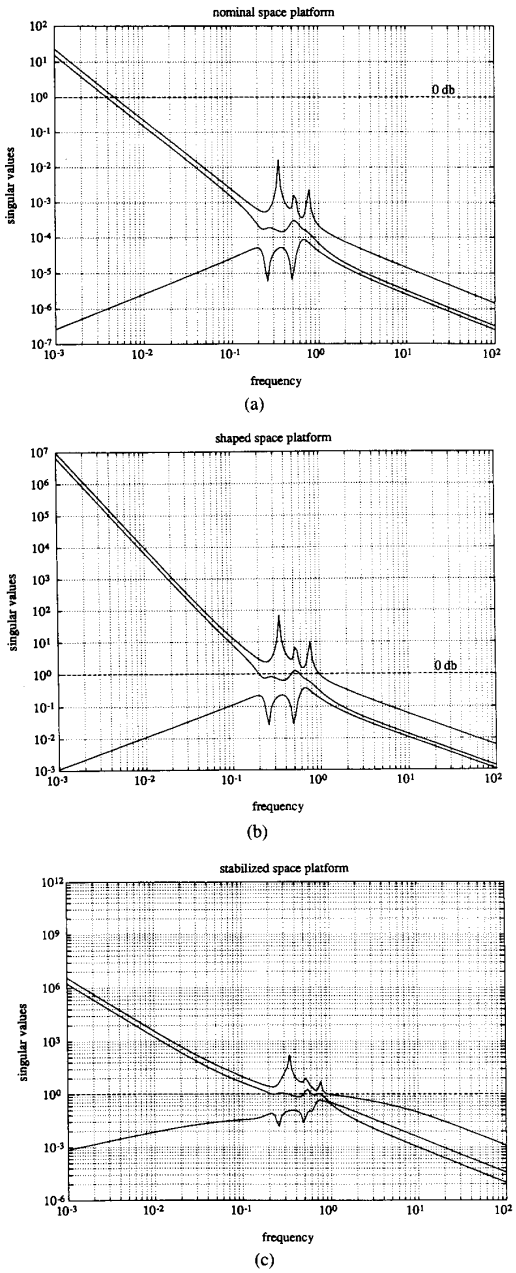

Fig. 5. Open-loop singular values. (a) Nominal plant. (b) Shaped plant. (c) Stabilized plant.

which had 12 states. Fig. 5(c) illustrates the open-loop singular values of the stabilized system KG.

D. Results

The results of the final design are presented here.

1) Robust Stability: Nominal and perturbed closed-loop systems were stable with minimum damping ratio of 12.6%-nominal and 8.6%-perturbed.

2) Disturbance Rejection: Maximum deflections for $0.1\,Nm$ step inputs on u_1 and u_2 were

$$y_1(\max) = 0.00075^\circ \ (0^\circ \text{ steady-state})$$
$$y_2(\max) = 0.00028^\circ \ (0^\circ \text{ steady-state}).$$

3) Control Effort: Maximum magnitudes (for $0.1\,Nm$ step inputs) of u_1 and u_2 were

$$u_1(\max) = 0.055Nm$$
$$u_2(\max) = 0.007Nm$$
$$u_3(\max) = 0.020N$$
$$u_4(\max) = 0.037N.$$

These compare favorably to the specifications set out in Section V-B.

E. Analysis of Results

Fig. 6 shows closed-loop frequency domain measures relevant to this design. In Fig. 6(a) the plot of $\bar{\sigma}((I - GK)^{-1}G)$ again highlights the effect of including integral action in the shaping function, giving zero steady-state transmission of input disturbance signals. The refinement of the disturbance rejection compared to the specified limits in this design was such that the major restriction in pointing accuracy is now the measurement system, rather than the feedback properties of the controller. See [16] for details. Fig. 6(b) shows $1/(\bar{\sigma}(GK(I - GK)^{-1}))$ and indicates that at low frequency, output multiplicative uncertainties of 100% of the plant magnitude can be tolerated, and in the plant crossover frequency region uncertainties of up to 30% can be tolerated. In Fig. 6(c) the plot of $1/(\bar{\sigma}(K(I - GK)^{-1}))$ shows that at high frequency, additive uncertainty well in excess of the plant magnitude can be tolerated. (It is common to interpret robust stability in terms of a combination of these two uncertainty descriptions.)

Next, it is interesting to compare the loop shapes obtained at different stages of the design. Comparing Fig. 5(b) and (c) it can be seen that the robust stabilization stage has not significantly altered the desired loop shape. In particular, note that the oscillatory plant modes are still present in the stabilized open-loop system. Cancellation of these modes by the controller can lead to poor robust stability and robust performance properties.

Finally, it is mentioned that additional analysis has demonstrated the robustness of the controller to the inclusion of spillover modes, and further investigations have shown that the highly desirable possibility of controlling the space platform only by means of the reaction wheels in the centerbody can be achieved. (Refer to [14] for details.)

Appendix
Proof of Results

Proof of Theorem 3.1: First note that $\underline{\sigma}(G_S) > \sqrt{\gamma^2 - 1}$ implies that

$$I + G_S G_S^* > \gamma^2 I$$

where the notation $A > (\geq) B$ implies $(A - B)$ positive (semi-)definite in the usual way. Further since $\tilde{M}_s \tilde{M}_s^* = I -$

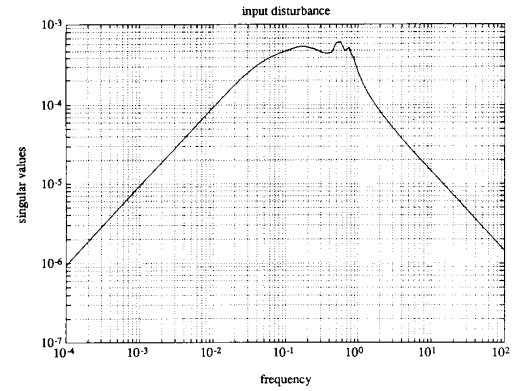

(a)

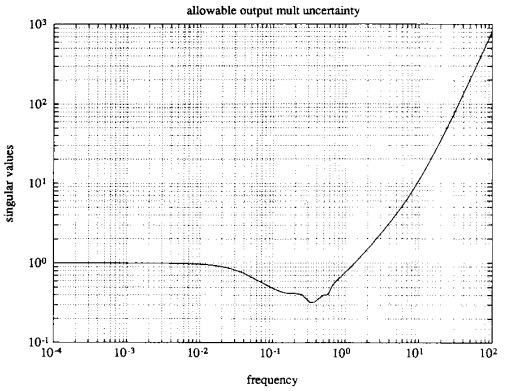

(b)

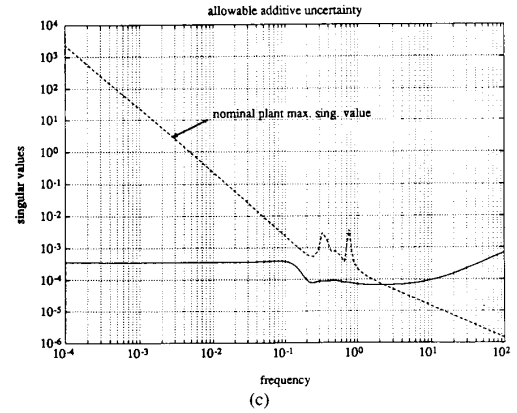

(c)

Fig. 6. Freqency domain measures: (a) $\bar{\sigma}((I - GK)^{-1}G)$. (b) $1/(\bar{\sigma}(GK(I - GK)^{-1}))$. (c) $1/(\bar{\sigma}(K(I - GK)^{-1}))$ and $\bar{\sigma}(G)$.

$\tilde{N}_s\tilde{N}_s^*$ and $G_S = \tilde{M}_s^{-1}\tilde{N}_s$, this implies that $\tilde{M}_s\tilde{M}_s^* < \gamma^{-2}I$.

$$\left\| \begin{bmatrix} K_\infty \\ I \end{bmatrix} (I - G_S K_\infty)^{-1} \tilde{M}_s^{-1} \right\|_\infty \leq \gamma$$

can be rewritten as

$$(I + K_\infty^* K_\infty) \leq \gamma^2 (I - K_\infty^* G_S^*)(\tilde{M}_s^* \tilde{M}_s)(I - G_S K_\infty). \tag{A.1}$$

We will next show that K_∞ is invertible. Suppose that there exists a x such that $K_\infty x = 0$, then $x^*(\text{A.1})x$ gives

$$\gamma^{-2} x^* x \leq x^* \tilde{M}_s^* \tilde{M}_s x$$

which implies that $x = 0$ since $\tilde{M}_s\tilde{M}_s^* < \gamma^{-2}I$, and hence K_∞ is invertible. Equation (A.1) can now be written as

$$\begin{aligned}
&(K_\infty^{*-1} K_\infty^{-1} + I) \\
&\quad \leq \gamma^2 (K_\infty^{*-1} - G_S^*)(I + G_S G_S^*)^{-1}(K_\infty^{-1} - G_S) \\
&\quad \Rightarrow K_\infty^{*-1}\left(I - \gamma^2 (I + G_S G_S^*)^{-1}\right) K_\infty^{-1} \\
&\qquad + \gamma^2 G_S^* (I + G_S G_S^*)^{-1} K_\infty^{-1} \\
&\qquad + \gamma^2 K_\infty^{*-1} (I + G_S G_S^*)^{-1} G_S \\
&\qquad + I - \gamma^2 G_S^* (I + G_S G_S^*)^{-1} G_S \leq 0.
\end{aligned}$$

This is a matrix quadratic function of K_∞^{-1}, and we note that the requirement

$$\left(I - \gamma^2 (I + G_S G_S^*)^{-1}\right) > 0 \tag{A.2}$$

is sufficient to enable completion of the square in terms of K_∞^{-1}. Therefore, assuming that condition (A.2) holds, we define W such that

$$(WW^*)^{-1} \triangleq \left(I - \gamma^2 (I + G_S G_S^*)^{-1}\right)$$

and completing the square in (A.2) yields

$$(K_\infty^{*-1} + N^*)(W^{*-1} W^{-1})(K_\infty^{-1} + N) \leq (\gamma^2 - 1) R^* R. \tag{A.3}$$

N is defined by

$$\begin{aligned}
N &\triangleq \gamma^2 W W^* (I + G_S G_S^*)^{-1} G_S \\
&= \gamma^2 G_S \left((1 - \gamma^2) I + G_S^* G_S\right)^{-1}
\end{aligned}$$

and R is defined such that

$$\begin{aligned}
&(\gamma^2 - 1) R^* R \\
&\quad = -I + \gamma^2 G_S^* (I + G_S G_S^*)^{-1} G_S \\
&\qquad + \gamma^4 G_S^* (I + G_S G_S^*)^{-1} W W^* (I + G_S G_S^*)^{-1} G_S \\
&\quad = -I + \gamma^2 G_S^* G_S (I + G_S^* G_S)^{-1} \\
&\qquad + \gamma^4 G_S^* G_S (I + G_S^* G_S)^{-1} \left((1 - \gamma^2) I + G_S^* G_S\right)^{-1} \\
&\quad = (I + G_S^* G_S)^{-1} \{ -(I + G_S^* G_S)\left((1 - \gamma^2) I \right. \\
&\qquad \left. + G_S^* G_S\right) + \gamma^2 G_S^* G_S \left((1 - \gamma^2) I + G_S^* G_S\right) \\
&\qquad + \gamma^4 G_S^* G_S \} \left((1 - \gamma^2) I + G_S^* G_S\right)^{-1} \\
&\quad = (\gamma^2 - 1)(I + G_S^* G_S)^{-1} \left\{ I + 2 G_S^* G_S + (G_S^* G_S)^2 \right\} \\
&\qquad \cdot \left((1 - \gamma^2) I + G_S^* G_S\right)^{-1} \\
&\quad = (\gamma^2 - 1)(I + G_S^* G_S)\left((1 - \gamma^2) I + G_S^* G_S\right)^{-1}.
\end{aligned} \tag{A.4}$$

Rearranging (A.3) we have the following condition on $\bar{\sigma}(K_\infty)$:

$$\begin{aligned}\bar{\sigma}\left(W^{-1}\left(K_\infty^{-1}+N\right)R^{-1}\right) &\le \left(\gamma^2-1\right)^{1/2}\\ \Rightarrow \bar{\sigma}\left(K_\infty^{-1}+N\right) &\le \left(\gamma^2-1\right)^{1/2}\bar{\sigma}(W)\bar{\sigma}(R)\\ \Rightarrow \underline{\sigma}(K_\infty) &\ge \left\{\left(\gamma^2-1\right)^{1/2}\bar{\sigma}(W)\bar{\sigma}(R)+\bar{\sigma}(N)\right\}^{-1}.\end{aligned} \tag{A.5}$$

To evaluate the appropriate bounds on $\bar{\sigma}(W)$, $\bar{\sigma}(N)$, and $\bar{\sigma}(R)$ we first let G_S have a singular value decomposition given by $G_S = Y\Sigma U^*$, where $\Sigma = \begin{bmatrix}\Sigma_1 & 0\\ 0 & 0\end{bmatrix}$ has the dimensions of the plant $(p \times m)$, $\Sigma_1 = \operatorname{diag}(\sigma_1, \cdots, \sigma_r)$, $i = 1, \cdots, r$, $r \le \min(m, p)$, and Y and U are square invertible functions of appropriate dimension satisfying $YY^* = I$ and $UU^* = I$. Then

$$\begin{aligned}WW^* &= \left(I+Y\Sigma^2Y^*\right)\left(\left(1-\gamma^2\right)I+Y\Sigma^2Y^*\right)^{-1}\\ &= Y\left(I+\Sigma^2\right)\left(\left(1-\gamma^2\right)I+\Sigma^2\right)^{-1}Y^*\end{aligned}$$

and

$$\sigma_i^2(W) = \lambda_i(WW^*) = \frac{1+\sigma_j^2(G_S)}{\left(1-\gamma^2\right)+\sigma_j^2(G_S)}.$$

It is then straightforward to verify that

$$\bar{\sigma}(W) = \left\{\frac{1+\underline{\sigma}^2(G_S)}{\underline{\sigma}^2(G_S)-\left(\gamma^2-1\right)}\right\}^{1/2}. \tag{A.6}$$

Note from (A.6) that the requirement $\underline{\sigma}(G_S) > (\gamma^2-1)^{1/2}$ is sufficient to guarantee that $(WW^*)^{-1} > 0$, and hence satisfy the assumption in (A.2).

Next note that, by inspection of (A.4) we have

$$\bar{\sigma}(R) = \bar{\sigma}(W) = \left\{\frac{1+\underline{\sigma}^2(G_S)}{\underline{\sigma}^2(G_S)-\left(\gamma^2-1\right)}\right\}^{1/2}. \tag{A.7}$$

Finally, using a singular value decomposition approach again, it is straightforward to verify that

$$\bar{\sigma}(N) = \frac{\gamma^2\underline{\sigma}(G_S)}{\underline{\sigma}^2(G_S)-\left(\gamma^2-1\right)}. \tag{A.8}$$

Using (A.6)–(A.8) in (A.5) we then have

$$\underline{\sigma}(K_\infty) \ge \left\{\frac{\left(\gamma^2-1\right)^{1/2}\left(1+\underline{\sigma}^2(G_S)\right)+\gamma^2\underline{\sigma}(G_S)}{\underline{\sigma}^2(G_S)-\left(\gamma^2-1\right)}\right\}^{-1}$$

giving the required result after canceling the factor $\underline{\sigma}(G_S) + \sqrt{\gamma^2-1}$. △△

Proof of Theorem 3.6: The proof of i) follows immediately from Vidyasagar [23, theorem 7.39], which shows that the requirement in (3.3) is sufficient *and* necessary for a single controller to stabilize all G_Δ in (3.2) subject to $\|[\Delta_N, \Delta_M]\|_\infty < \epsilon$.

The proofs for ii) and iii) are, in the main part, analogous to the proofs of Theorems 3.1 and 3.3. The procedure is therefore only sketched here.

To prove ii) we note by (3.9) that, at frequency ω_o, there exists a vector x such that

$$\begin{aligned}&x^*\left(I+K_a^*K_a\right)x\\ &\quad\ge \gamma_{\min}^2x^*\left(I-K_a^*G_S^*\right)\left(I+G_SG_S^*\right)^{-1}\left(I-G_SK_a\right)x\\ &\quad\Rightarrow x^*\Big\{K_a^*\left(I-\gamma_{\min}^2G_S^*\left(I+G_SG_S^*\right)^{-1}G_S\right)K_a\\ &\qquad+\gamma_{\min}^2K_a^*G_S^*\left(I+G_SG_S^*\right)^{-1}\\ &\qquad+\gamma_{\min}^2\left(I+G_SG_S^*\right)^{-1}G_SK_a\\ &\qquad+I-\gamma_{\min}^2\left(I+G_SG_S^*\right)^{-1}\Big\}x \ge 0.\end{aligned} \tag{A.9}$$

We again complete the squares in terms of K_a, noting that

$$\left(I-\gamma_{\min}^2G_S^*\left(I+G_SG_S^*\right)^{-1}G_S\right) < 0$$

is a sufficient requirement, and noting further that this is satisfied if

$$\underline{\sigma}(G_S) > \left(\gamma_{\min}^2-1\right)^{-1/2}.$$

Analogously to the proof of Theorem A.3, we then have, from (A.9),

$$\begin{aligned}&x^*\left\{\left(K_a^*-M_1^*\right)\left(V_1^{*-1}V_1^{-1}\right)\left(K_a-M_1\right)\right\}x\\ &\qquad\le \left(\gamma_{\min}^2-1\right)x^*Y_1^*Y_1x\end{aligned} \tag{A.10}$$

where V_1, M_1, and W_1 satisfy

$$\begin{aligned}\left(V_1^{*-1}V_1^{-1}\right) &= \left(I-\gamma_{\min}^2G_S^*\left(I+G_SG_S^*\right)^{-1}G_S\right)\\ Y_1^*Y_1 &= \left(V_1^{*-1}V_1^{-1}\right)\\ M_1 &= \gamma_{\min}^2V_1V_1^*G_S^*\left(I+G_SG_S^*\right)^{-1}.\end{aligned}$$

By (A.10) we then have that

$$\begin{aligned}\left\|V_1^{-1}\left(K_a-M_1\right)x\right\|_2 &\le \left(\gamma_{\min}^2-1\right)^{1/2}\left\|Y_1x\right\|_2\\ \Rightarrow \bar{\sigma}\left(V_1^{-1}\right)\underline{\sigma}\left(K_a-M_1\right) &\le \left(\gamma_{\min}^2-1\right)^{1/2}\bar{\sigma}(Y_1)\\ \Rightarrow \underline{\sigma}(K_a) &\le \left(\gamma_{\min}^2-1\right)^{1/2}\bar{\sigma}(Y_1)\bar{\sigma}(V_1)+\bar{\sigma}(M_1).\end{aligned} \tag{A.11}$$

It is then simple to verify that

$$\bar{\sigma}(V_1) = \bar{\sigma}(Y_1) = \left\{\frac{1+\underline{\sigma}^2(G_S)}{\left(\gamma_{\min}^2-1\right)\underline{\sigma}^2(G_S)-1}\right\}^{1/2} \tag{A.12}$$

and

$$\bar{\sigma}(M_1) = \frac{\gamma_{\min}^2\underline{\sigma}(G_S)}{\left(\gamma_{\min}^2-1\right)\underline{\sigma}^2(G_S)-1} \tag{A.13}$$

and (A.12) and (A.13) in (A.11) then completes the proof of ii).

The proof of iii) can be constructed in an identical manner. △△

REFERENCES

[1] H. Bode, *Network Analysis & Feedback Amplifier Design*. New York: Van Nostrand, 1945.

[2] J. Doyle, "Analysis of feedback systems with structured uncertainties," *IEE Proc.*, vol. 129-D, no. 6, pp. 242-250, 1982.

[3] J. Doyle and G. Stein, "Multivariable feedback design: Concepts for a classical modern synthesis," *IEEE Trans. Automat. Contr.*, vol. AC-26, no. 1, pp. 4-16, 1981.

[4] B. Francis, *A Course in H_∞ Control Theory*. New York: Springer-Verlag, 1987.

[5] J. Freudenberg and D. Looze, *Frequency Domain Properties of Scalar and Multivariable Feedback Systems*. New York: Springer-Verlag, 1987.

[6] T. T. Georgiou and M. C. Smith, "Optimal robustness in the gap metric," *IEEE Trans. Automat. Contr.*, vol. 35, pp. 673-686, June 1990.

[7] K. Glover and D. McFarlane, "Robust stabilization of normalized coprime factors: An explicit H_∞ solution," in *Proc. 1988 Amer. Contr. Conf.*, Atlanta, GA, 1988.

[8] ——, "Robust stabilization of normalized coprime factor plant descriptions with H_∞-bounded uncertainty," *IEEE Trans. Auto. Contr.*, vol. 34, pp. 821-830, Aug. 1989.

[9] I. Horowitz, *Synthesis of Feedback Systems*. New York: Academic, 1963.

[10] Y. S. Hung and A. MacFarlane, *Multivariable Feedback: A Quasi-Classical Approach*. New York: Springer-Verlag.

[11] H. Kwakernaak and R. Sivan, *Linear Optimal Control Systems*. New York: Wiley, 1972.

[12] D. McFarlane, K. Glover, and M. Noton, "Robust stabilization of a flexible space-platform: An H_∞ coprime factorization approach," in *Proc. Contr. 88', IEE Conf.*, Oxford, expanded in CUED Internal Rep. CUED/F-INFENG/TR.5.), 1988.

[13] D. McFarlane and K. Glover, "An H_∞ design procedure using robust stabilization of normalized coprime factors," in *Proc. 1988 Conf. Decision Contr.*, Austin, TX, 1988.

[14] ——, "Robust controller design using normalised coprime factor plant descriptions, (Lecture Notes in Control and Information Sciences, Vol. 138). New York: Springer Verlag, 1989.

[15] J. Maciejowski, *Multivariable Feedback Design*. Reading, MA: Addison-Wesley, 1989.

[16] M. Noton, "H_∞ control design for complex space structures," British Aerospace, Space and Commun. Division, Bristol, U.K., Rep. TR9047, 1989.

[17] M. Safonov, G. Hartmann, and A. Laub, "Feedback properties of multivariable systems: The role and use of the return difference matrix," *IEEE Trans. Automat. Contr.*, vol. 21, pp. 47-63, 1981.

[18] M. Safonov and R. Chiang, "CACSD using the state space L_∞ theory —A design example," *IEEE Trans. Automat. Contr.*, vol. 33, pp. 477-479, May 1988.

[19] M. Safonov, "Optimal H_∞ synthesis of robust controllers for systems with structured uncertainty," in *Proc. CDC*, Athens, Greece, 1986.

[20] J. Sefton and K. Glover, "Pole/zero cancellations in the general H_∞ problem with reference to a two block design," *Syst. Contr. Lett.*, vol. 14, no. 3, 1990.

[21] G. Stein and M. Athans, "The LQG/LTR procedure for multivariable feedback design," *IEEE Trans. Automat. Contr.*, vol. 32, pp. 105-114, 1987.

[22] M. Vidyasagar, "The graph metric for unstable plants and robustness estimates for feedback stability," *IEEE Trans. Automat. Contr.*, vol. 29, pp. 403-417, 1984.

[23] ——, *Control System Synthesis: A Coprime Factorization Approach*. Cambridge, MA: M.I.T. Press, 1985.

[24] M. Vidyasagar and H. Kimura, "Robust controllers for uncertain linear multivariable systems," *Automatica*, pp. 85-94, 1986.

[25] G. Zames, "Feedback and optimality sensitivity: Model reference transformations, multiplicative seminorms, and approximate inverses," *IEEE Trans. Automat. Contr.*, vol. 26, pp. 301-320, 1981.

[26] Z. Zhang and J. Freudenberg, "Loop transfer recovery for nonminimum phase plants," *IEEE Trans. Automat. Contr.*, vol. 35, pp. 547-553, 1990.

Duncan McFarlane (S'87-M'88) was born in Melbourne, Australia, in 1963. He received the B. Eng. degree in mechanical engineering from the University of Melbourne, Melbourne, Australia, in 1984, and the Ph.D. degree in control from the University of Cambridge, Cambridge, England, in 1988.

He has been employed by BHP Co. Ltd., Australia, since 1980, and is currently coordinator of Automation Technology Research at BHP Research, Melbourne Laboratories, Melbourne, Australia. His research interests include robust filtering and control, process automation, modeling, neural networks, and applications of control in the steel and minerals industries.

Keith Glover (S'71-M'73-SM'90) was born in Bromley, Kent, England, in 1946. He received the B.Sc.(Eng.) degree from Imperial College, London, in 1967, and the S.M., E.E., and Ph.D. degrees from the Massachusetts Institute of Technology, Cambridge, in 1971, 1971, and 1973, respectively, all in electrical engineering.

From 1967 to 1969 he was a Development Engineer with the Marconi Company. From 1973 to 1976 he was on the faculty of the University of Southern California, Los Angeles. Since 1976 he has been with the Department of Engineering, University of Cambridge, U.K., where his present position is Professor of Engineering. His current research interests include linear systems, model approximation, robust control, and various applications.

Dr. Glover was a Kennedy Fellow at M.I.T. from 1969-1971 and a Visiting Fellow at the Australian National University, in 1983-1984. He was a corecipient of the AACC O. Hugo Shuck Award at the 1983 ACC; of the George S. Axelby Outstanding Paper Award for 1990; and of the IEEE W. G. R. Baker Prize Award for 1991.